Extraction of the First-Arriving-Signal and Fundamental Flexural Guided Wave Using a Radon Transform Based Approach Applied to Ultrasonic Characterization of Cortical Bone

Feiyao Ling [1], Dongmei Xu [1], Kailiang Xu[1,2*], Qi Chen[1], Tho N.H.T. Tran [2], Petro Moilanen[3], Jean-Gabriel Minonzio[4,5], Dean Ta[1,2]
[1] Center for Biomedical Engineering, Fudan University, Shanghai, China
[2] Academy for Engineering and Technology, Fudan University, Shanghai, China
[3] Department of Physics, University of Helsinki, Helsinki, Finland
[4] Escuela de Ingeniería Informática, Universidad de Valparaíso, Valparaíso, Chile
[5]Centro de Investigación y Desarrollo en Ingeniería en Salud, Universidad de Valparaíso, Valparaíso, Chile

***Abstract*—Ultrasonic guided waves have been used for characterizing cortical bone. However, multimode ultrasound signals bring difficulty in signal processing, making it challenging to extract the first arriving signals (FAS) and the individual mode components for cortical bone characterization. To overcome such a limitation, a feasibility study of cortical bone evaluation utilizing the Radon transform based signal extraction method is introduced in this paper. Forward and inverse Radon transform pair is applied to increase the signal-to-noise ratio of the ultrasonic signals collected from a bovine bone plate. Based on the known velocity ranges, the regions of interest in the intercept-slowness domain are extracted to obtain the FAS and the fundamental flexural guided wave (A0 mode) signals. Compared to the true geometric and elastic parameters, the proposed method enables to retrieve the cortical thickness, longitudinal and transverse velocities, which suggests a potential application of bone characterization.**

Keywords—Ultrasonic guided waves, Radon transform, cortical bone, axial transmission, waveguide parameter estimation

I. Introduction

Ultrasonic guided waves have been used for characterizing long cortical bones for their sensitivity in both geometric and elastic properties [1-4]. Compared to the Dual-energy X-ray absorptiometry (DXA), the clinical gold standard in evaluating the patients at risk of fracture [5-6], ultrasound-based diagnosis methods have advantages in smaller devices, better portability and absence of ionizing radiation. Axial transmission technique has been established for measuring the ultrasonic signals propagating in the cortical shell of long bones [6-9]. The cortical bone is usually considered as a free boundary layered structure [10-11] and ultrasonic Lamb waves theory can thus be used to interpret waveguides developed in the cortical bone. Studies based on the first arriving signals (FAS) and the fundamental flexural guided waves (A0 waves) [7-8,12-13] have been performed for estimating cortical thickness and elasticity for the long bones. However, multimode guided signals bring difficulty in signal processing, making it challenging to characterize cortical bone properties [4,14-15].

Inverse methods based on broadband dispersion curves [16] have been proposed to evaluate bone thickness. Singular vector decomposition (SVD) was introduced to improve the signal-to-noise ratio (SNR) and extract high-resolution dispersion curves [17]. Methods have been proposed to achieve a higher wavenumber resolution, such as sparse SVD (S-SVD) [18], Radon transform (RT) [19], and estimation of signal parameters via rotation invariant technique (ESPRIT) [20]. However, it is relatively difficult to excite broadband multimode guided waves, because only the modes propagating at a limited range of phase velocity can be excited according to Snell's law [21]. In addition, the influences of soft tissue lead to a challenging model fitting in the inverse schemes [22].

Mode separation methods have also been proposed to extract single mode ultrasound components for cortical bone characterization. In single-channel signal processing, crazy-climber algorithm has been applied to separate ridges of the single mode signals in the time-frequency domain [20]. Due to the dispersion characteristic of Lamb waves, dispersion compensation method has been proposed to separate S0 and A0 modes from multimode signals received from a steel plate [24]. Nevertheless, limited information of the dispersive properties can be recorded in single channel signals. In multi-channel evaluation, linear Radon transform has been applied to the *in vitro* data to increase the SNR and separate different wave components [25]. By projecting distance-time domain signals to intercept-slowness (τ–p) domain where the slowness p is the reciprocal of the phase velocity and the intercept τ is the offset of the time [26], linear Radon transform provides a solution to separate different signal components by their velocity difference. Recently, dispersive Radon transform (DRT), which projects the multichannel temporal signals to the parameter space of interest, has been proposed to separate a single mode from multimode guided waves, and therefore estimate cortical thickness of *ex vivo* human radius [27].

Motivated by the previous studies, a cortical bone evaluation method based on signal extraction by Radon transform is introduced in this paper. Multichannel ultrasound guided waves were collected from a bovine bone plate. Radon transform was utilized to increase the SNR and project the temporal guided wave signals to τ–p domain. Since the FAS are the fastest wave components and A0 waves are the slowest, single mode signals can be extracted in the τ–p domain by their velocity difference. The thickness and elastic

Project supported by National Natural Science Foundation of China (Grant Nos. 11974081, 11827808), Natural Science Foundation of Shanghai, China (No. 19ZR1402700), Shanghai Rising Star Program, China (Grant No. 20QC1400200), and Shanghai Academic Research Leader Program, China (No. 19XD1400500).

Corresponding author: Kailiang Xu, xukl@fudan.edu.cn

2021 IEEE International Ultrasonics Symposium (IUS) | 978-1-6654-0355-9/21/$31.00 ©2021 IEEE | DOI: 10.1109/IUS52206.2021.9593783

parameters of the bone were acquired through an inverse approach based on the Rayleigh-Lamb wave equation, where the best match parameters were obtained by minimizing the cost function which describes the difference between the extracted and theoretical dispersion curves.

II. Materials And Methods

A. Ultrasonic Lamb Waves in Cortical Bone

The guided waves that propagate along a solid plate with free boundaries are called the Lamb waves, which can be classified as symmetric and anti-symmetric modes according to their displacement patterns. For an isotropic plate with a thickness of *2h*, the dispersion curves of the Lamb waves can be calculated according to the Rayleigh-Lamb equations

$$\text{Symmetric modes: } \frac{\tan(qh)}{\tan(ph)} = \frac{-4k^2pq}{(q^2-k^2)^2}, \quad (1a)$$

$$\text{Anti-symmetric modes: } \frac{\tan(qh)}{\tan(ph)} = \frac{-(q^2-k^2)^2}{4k^2pq}, \quad (1b)$$

$$p^2 = \omega^2/C_L^2 - k^2,\ p^2 = \omega^2/C_T^2 - k^2, \quad (1c)$$

where k is the wavenumber, and C_L and C_T stands for the longitudinal and transverse velocities of the plate, respectively [28-29].

B. Linear Radon Transform

If a set of multichannel signals $d(t, r_n)$ are collected at different propagation distances $r_0, r_1, \ldots, r_{Nr-1}$, where t represents time, the discrete forward Radon transform can be defined as

$$m(\tau, p_k) = \sum_{n=0}^{N_r-1} d(t = \tau + p_k r_n, r_n),\ k = 0, 1, \ldots, N_p - 1, \quad (2a)$$

and the inverse Radon transform can be defined as

$$d(t, r_n) = \sum_{k=0}^{N_p-1} m(\tau = t - p_k r_n, p_k),\ n = 0, 1, \ldots, N_r - 1, \quad (2b)$$

where N_P is the number of slowness sampling points and N_r is the number of distance sampling points. The term $m(\tau, p_k)$ in Eq. (2a) and (2b) is a $\tau-p$ set, where τ stands for the temporal intercept and p stands for the slowness which is the inverse of the phase velocity. Frequency domain is introduced to simplify the calculation, and Eq. (2b) can be written as

$$D(f, r_n) = \sum_{k=0}^{N_p-1} M(f, p_k) e^{-i2\pi f p_k r_n}. \quad (3)$$

Rewritten (3) in matrix format as

$$\boldsymbol{D} = \boldsymbol{LM}, \quad (4)$$

where $\boldsymbol{L}$ is the Radon operator noted as

$$\boldsymbol{L} = \begin{pmatrix} e^{-j2\pi f p_1 r_1} & \cdots & e^{-j\,2\,\pi f\, p_{N_p} r_1} \\ \vdots & \ddots & \vdots \\ e^{-j\,2\pi f p_1 r_{N_r}} & \cdots & e^{-j\,2\pi f\, p_{N_p} r_{N_r}} \end{pmatrix}. \quad (5)$$

The least-squares solution to Eq. (4) can be obtained by minimizing the cost function [30]

$$J = ||\boldsymbol{D} - \boldsymbol{LM}||_2^2 + \mu Q(\boldsymbol{M}), \quad (6)$$

where $Q(\boldsymbol{M})$ is the penalty term and μ is the Lagrange multiplier which balances the data fidelity and sparse penalty term. A common choice of the penalty term is quadratic norm or l_2 norm, which is $Q(\boldsymbol{M})=||\boldsymbol{M}||^2$. Hence, least-square solution can be obtained as

$$\tilde{\boldsymbol{M}} = (\boldsymbol{L}^H\boldsymbol{L} + \mu\boldsymbol{I})^{-1}\boldsymbol{L}^H\boldsymbol{D}, \quad (7)$$

where $\boldsymbol{L}^H$ is the complex conjugate transpose, or Hermitian conjugate, of $\boldsymbol{L}$.

C. Experiment Setup

The experiment is performed with a 1 MHz linear array probe (Wisonic, Shenzhen, China) with 128 channels connected to a multichannel ultrasound platform (Vantage-128, Verasonics, WA, USA). The −6 dB bandwidth of the probe is 0.5 – 1.5 MHz, and the pitch size is 0.675 mm. The ultrasonic excitation is generated by the first 5 emitters with the central frequency of 1 MHz and the received signals are collected from the last 64 receivers. The ultrasound gel is used to ensure the coupling between the probe and the bone plate. The 1.8 mm-thick bovine bone plate has the longitudinal wave speed of 4.00 mm·μs^{-1} and the transverse wave speed of 1.97 mm·μs^{-1} according to the previous report [31].

III. Results

A. Radon Transform Based Denoising

The original received signals and dispersion energy distribution using Radon transform are displayed in Figs. 1 (a) and (b), respectively. Denoised signals are obtained by performing a pair of Radon transforms (forward and inverse) to the received signals [32]. To demonstrate the denoising results clearly, signals at the distance of 48.6, 51.3 and 54 mm are displayed in Fig. 1 (c), where the black lines depict the received signals and the red lines depict the denoised signals. Comparing the received signals and the denoised signals in the red box, the small disturbance are smoothed, indicating an increase of the SNR through a Radon transform pair.

B. FAS and A0 Waves Extraction

The denoised signals in Fig. 2 (a) are projected to the τ–p domain with the Radon transform, and based on the known velocity ranges, the regions of interest in the τ–p domain are filtered to obtain the FAS and the A0 waves. Since the FAS are the fastest wave components, the window bounded by p in 0.2 ~ 0.33 μs·mm^{-1} and τ in 8.8 ~ 14.5 μs, which is the smaller red box in Fig. 2 (b), is applied to reconstruct the FAS in Fig. 2 (c). Similarly, the A0 waves, which are the slowest guided wave mode, are windowed by the larger red box in Fig. 2 (b) with the slowness ranges of above 0.55 μs·mm^{-1} and intercept ranges of 38 ~ 42.25 μs, and the reconstructed A0 waves are shown in Fig. 2 (e). The dispersive energy distribution of the FAS and A0 waves are obtained by Radon transform in Fig. 2 (d) and (f), respectively. The extracted A0 waves are in consistency with the theoretical dispersion curve of the A0 wave plotted as the red line in Fig. 2 (f). By picking the maximum value in the FAS region, the slowness of FAS at the frequency of 1 MHz can be obtained as 0.26 μs·mm^{-1}, from which its velocity can be calculated as 3.85 mm·μs^{-1}.

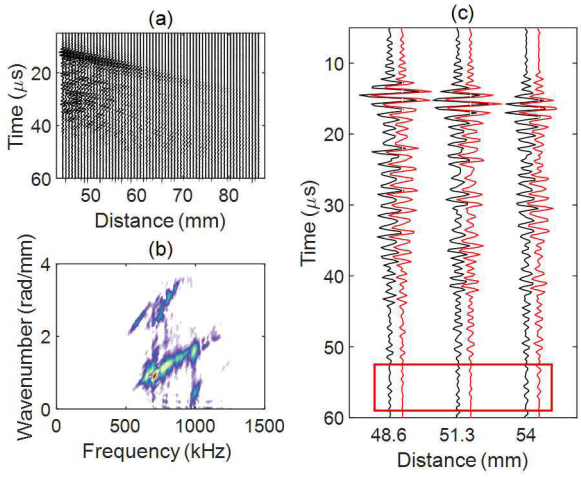

Fig. 1. Denoising results of the received signals based on Radon transform pair. The original received signals are plotted in (a), of which the dispersion energy distributions are shown in (b), and the denoising results are displayed in (c) with the original signals in black and denoised signals in red.

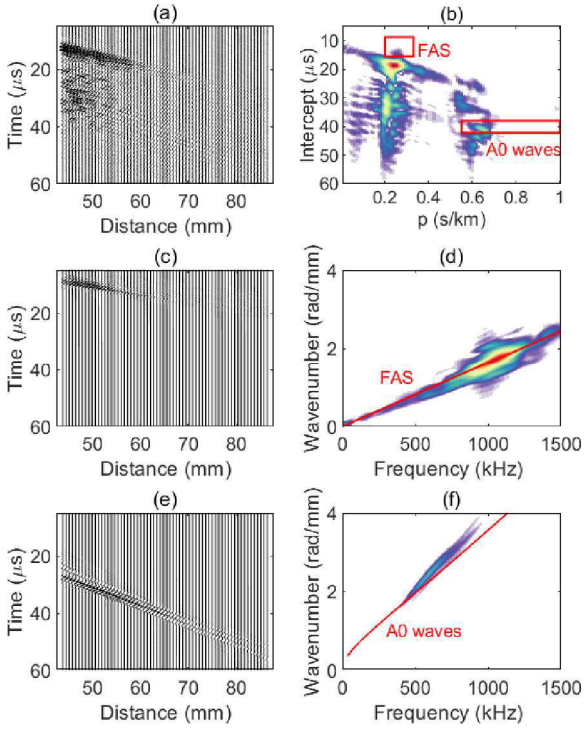

Fig. 2. FAS and A0 waves extraction results based on Radon transform. The smoothed signals are displayed in (a), and its $p-\tau$ projections are shown in (b), where the red boxes represent the filtered region of FAS and A0 waves, respectively. The extracted FAS are plotted in (c) with the dispersion energy in (d), and the extracted A0 waves are plotted in (d) with the dispersion energy in (e) where the red line is the theoretical dispersion curve of A0 mode.

C. *Evaluations of Thickness and Elastic Properties*

An inverse scheme is used to estimate the model parameter θ which is a vector consists of plate thickness Th and transverse velocity C_T. Since the central frequency of the excitation f_0 and the FAS speed V_{FAS} are known, the longitudinal velocity C_L of the bovine bone plate can be estimated from thickness Th according to the polynomial fitting based on the previous numerical simulation studies [33-34]

$$P(C_L, Th, V_{FAS}, f_0) = 0. \quad (8)$$

According to Eq. (1b), (1c) and (8), the theoretical dispersion curve in the f–k plane under parameters θ can therefore be written as

$$[f(\theta), k(\theta)] = D(\theta, V_{FAS}, f_0) \quad (9)$$

The best match parameters are estimated by minimizing the cost function $F(\theta)$ which describes the weighted Euclidean distance between the extracted dispersive distribution and the theoretical dispersion curves. Hence,

$$F(\theta) = \sum_{j=1}^{N} E(f_j, k_j) \cdot \sqrt{\left(\frac{f_j - f(\theta)}{f_{max}}\right)^2 + \left(\frac{k_j - k(\theta)}{k_{max}}\right)^2}, \quad (10)$$

where N is the total number of the experiment data and $E(f, k)$ is the amplitude of the dispersive energy distribution on the f–k plane.

The inversion ranges of thickness and transverse velocity are 1.75 ~ 1.85 mm and 1.61 ~ 2.40 mm·μs^{-1}, respectively. The results from (10) based on the A0 mode dispersion curve are displayed in the Fig. 3. The inverse results of the longitudinal wave speed, transverse wave speed and thickness were 3.99 mm·μs^{-1}, 1.79 mm·μs^{-1} and 1.825 mm, respectively, which were consistent with the actual values of the bovine bone plate mentioned above.

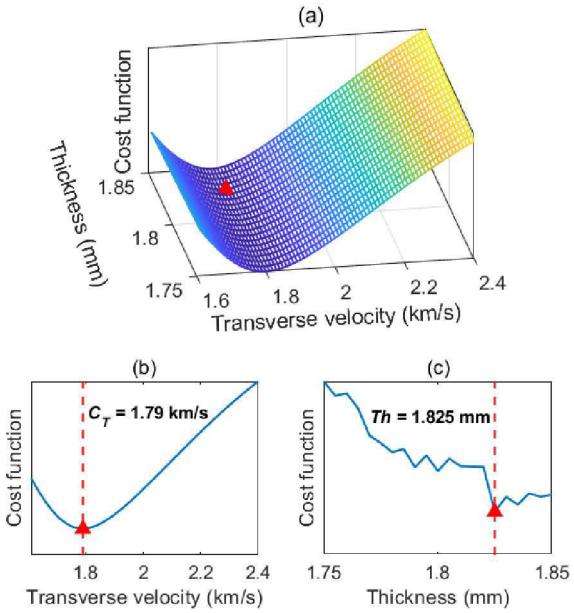

Fig. 3. The results of the cost function. The cost function values in the inversion ranges are shown in (a) where the triangle point is the best match point, while (b) and (c) depict the cost function values at the best matching thickness and the transverse velocity, respectively.

IV. Conclusion

In this study, a Radon transform based method was introduced to extract the FAS and A0 waves. With the prior knowledge of approximate velocity ranges, the proposed method was capable of extracting FAS and FFGW in the τ–p domain. According to the extraction results, the thickness and the elastic properties of the bovine bone plate were evaluated, showing high consistency with the actual values. The results indicate that the proposed method has a potential in

evaluating geometric and elastic properties of long cortical bones based on multichannel ultrasound techniques. The performance on extracting other modes of Lamb waves and the results of *in vivo* experiments of this method should be further investigated.

REFERENCES

[1] M. Ducousso, A. Dalodiere, and A. Baillard, "Evaluation of the thermal aging of aeronautical composite materials using Lamb waves," Ultrasonics, vol. 94, pp. 174–182, 2019.

[2] Z. Liu, K. Xu, D. Li, D. Ta, and W. Wang, "Automatic mode extraction of ultrasonic guided waves using synchrosqueezed wavelet transform," Ultrasonics, vol. 99, pp. 105948, 2019.

[3] X. Cao, L. Zeng, and J. Lin, "Lamb wave mode decomposition and reconstruction based on the viscoelastic propagation model," Structural Health Monitoring, vol. 20(1), pp. 25-45, 2021.

[4] J.G. Minonzio, N. Bochud, Q. Vallet, Y. Bala, D. Ramiandrisoa, H. Follet, D. mitton, and P. Laugier, "Bone cortical thickness and porosity assessment using ultrasound guided waves: An ex vivo validation study," Bone, vol. 116, pp. 111-119, 2018.

[5] E. Siris, and P. D. Delmas, "Assessment of 10-year absolute fracture risk: a new paradigm with worldwide application," Osteoporosis International, vol. 19(4), pp. 383-384, 2008.

[6] J.G. Minonzio, N. Bochud, Q. Vallet, D. Ramiandrisoa, A. Etcheto, K. Briot, S. Kolta, C. Roux, and P. Laugier, "Ultrasound - Based Estimates of Cortical Bone Thickness and Porosity Are Associated With Nontraumatic Fractures in Postmenopausal Women: A Pilot Study." Journal of Bone and Mineral Research, vol. 34(9), pp. 1585-1596, 2019.

[7] J. Schneider, D. Ramiandrisoa, G. Armbrecht, Z. Ritter, D. Felsenberg, K. Raum, and J.G. Minonzio, "In vivo measurements of cortical thickness and porosity at the proximal third of the tibia using guided waves: Comparison with site-matched peripheral quantitative computed tomography and distal high-resolution peripheral quantitative computed tomography," Ultrasound in Medicine and Biology, vol. 45(5) ,pp. 1234-1242, 2019.

[8] J. Schneider, G. Iori, D. Ramiandrisoa, M. Hammami, M. Grasel, C. Chappard, R. Barkmann, P. Laugier, Q. Grimal, J.G. Minonzio, and K. Raum, "Ex vivo cortical porosity and thickness predictions at the tibia using full-spectrum ultrasonic guided-wave analysis," Archives of Osteoporosis, vol. 14(1), pp. 1-11, 2019.

[9] Y. Li, K. Xu, Y. Li, F. Xu, D. Ta, and W. Wang, "Deep Learning Analysis of Ultrasonic Guided Waves for Cortical Bone Characterization," IEEE Transactions on Ultrasonics, Ferroelectrics, and Frequency Control, vol. 68(4), pp. 935-951, 2021.

[10] F. Lefebvre, Y. Deblock, P. Campistron, D. Ahite, and J.J. Fabre, "Development of a new ultrasonic technique for bone and biomaterials in vitro characterization," Journal of Biomedical Materials Research, vol. 63(4), pp. 441-446, 2002.

[11] J.G. Minonzio, J. Foiret, P. Moilanen, J. Pirhonen, Z. Zhao, M. Talmant, J. Timonen, and P. Laugier, "A free plate model can predict guided modes propagating in tubular bone-mimicking phantoms," The Journal of the Acoustical Society of America, vol. 137(1), pp. EL98-EL104, 2015.

[12] A.J. Foldes, A. Rimon, D.D. Keinan, and M.M. Popovtzer, "Quantitative ultrasound of the tibia: a novel approach for assessment of bone status," Bone, vol. 17(4), pp. 363-367, 1995.

[13] P.H.F. Nicholson, P. Moilanen, T. Karkkainen, J. Timonen, and S. Cheng, "Guided ultrasonic waves in long bones: modelling, experiment and in vivo application," Physiological Measurement, vol. 23(4), pp. 755, 2002.

[14] N. Bochud, J. Laurent, F. Bruno, D. Royer, and C. Prada, "Towards real-time assessment of anisotropic plate properties using elastic guided waves," The Journal of the Acoustical Society of America, vol. 143(2), pp. 1138, 2018.

[15] G. Renaud, P. Clouzet, D. Cassereau, and M. Talmant, "Measuring anisotropy of elastic wave velocity with ultrasound imaging and an autofocus method: application to cortical bone," Physics in Medicine and Biology, vol. 65(23), pp. 235016, 2020.

[16] N. Bochud, Q. Vallet, Y. Bala, H. Follet, J. G. Minonzio, and P. Laugier, "Genetic algorithms-based inversion of multimode guided waves for cortical bone characterization," Physics in Medicine and Biology, vol. 61(19), pp. 6953-6974, 2016.

[17] J.G. Minonzio, M. Talmant, and P. Laugier. "Guided wave phase velocity measurement using multi-emitter and multi-receiver arrays in the axial transmission configuration," The Journal of the Acoustical Society of America, vol. 127(5), pp. 2913-2919, 2010.

[18] K. Xu, J.G. Minonzio, D. Ta, B. Hu, W. Wang, and P. Laugier, "Sparse SVD method for high-resolution extraction of the dispersion curves of ultrasonic guided waves," IEEE Transactions on Ultrasonics, Ferroelectrics, and Frequency Control vol. 63(10), pp. 1514-1524, 2016.

[19] T.N.H.T. Tran, K.C.T. Nguyen, M.D. Sacchi, and L.H. Le, "Imaging ultrasonic dispersive guided wave energy in long bones using linear radon transform," Ultrasound in Medicine and Biology, vol. 40(11) ,pp. 2715-2727, 2014.

[20] Q. Chen, K. Xu, and D. Ta, "High-resolution Lamb waves dispersion curves estimation and elastic property inversion," Ultrasonics, vol. 115, pp. 106427, 2021.

[21] K. C. Nguyen, L. H. Le, T. N. Tran, M. D. Sacchi, and E. H. Lou, "Excitation of ultrasonic Lamb waves using a phased array system with two array probes: phantom and in vitro bone studies," Ultrasonics, vol. 54(5), pp. 1178-85, 2014.

[22] T.N.H.T. Tran, L. Stieglitz, Yu J. Gu, Lawrence H. Le, "Analysis of ultrasonic waves propagating in a bone plate over a water half-space with and without overlying soft tissue," Ultrasound in Medicine and Biology, Vol. 39(12), pp. 2422-2430, 2013.

[23] K. Xu, D. Ta, and W. Wang, "Multiridge-based analysis for separating individual modes from multimodal guided wave signals in long bones," IEEE Transactions on Ultrasonics, Ferroelectrics, and Frequency Control, vol. 57(11), pp. 2480-90, 2010.

[24] K. Xu, D. Ta, P. Moilanen, and W. Wang, "Mode separation of Lamb waves based on dispersion compensation method," The Journal of the Acoustical Society of America, vol. 131(4), pp. 2714-22, 2012.

[25] T.N.H.T Tran, L.H. Le, M.D. Sacchi, V.H. Nguyen, and E.H. Lou, "Multichannel filtering and reconstruction of ultrasonic guided wave fields using time intercept-slowness transform," The Journal of the Acoustical Society of America, vol. 136(1), pp. 248-259, 2014.

[26] R.A. Phinney, K.R. Chowdhury, and L.N. Frazer, "Transformation and analysis of record sections," Journal of Geophysical Research: Solid Earth, vol. 86(B1), pp. 359-377, 1981.

[27] K. Xu, P. Laugier, and J. G. Minonzio, "Dispersive Radon transform," The Journal of the Acoustical Society of America, vol. 143(5), pp. 2729-2743, 2018.

[28] J.L. Rose, Ultrasonic Guided Waves in Solid Media. Cambridge University Press, 2014.

[29] K. Xu, D. Ta, B. Hu, P. Laugier, and W. Wang, "Wideband dispersion reversal of Lamb waves," IEEE Transactions on Ultrasonics, Ferroelectrics, and Frequency Control, vol. 61(6), pp. 997-1005, 2014.

[30] M. D. Sacchi, "Reweighting strategies in seismic deconvolution," Geophysical Journal International, vol. 129(3), pp. 651-656, 1997.

[31] L. H. Le, Y. J. Gu, Y. P. Li, and C. Zhang, "Probing long bones with ultrasonic body waves," Applied Physics Letters, vol. 96, no. 11, Mar 15, 2010.

[32] J. I. Sabbione, M. D. Sacchi, and D. R. Velis, "Radon transform-based microseismic event detection and signal-to-noise ratio enhancement," Journal of Applied Geophysics, vol. 113, pp. 51-63, 2015.

[33] E. Bossy, M. Talmant, and P. Laugier, "Effect of bone cortical thickness on velocity measurements using ultrasonic axial transmission: a 2D simulation study," The Journal of the Acoustical Society of America, vol. 112(1), pp. 297-307, 2002.

[34] E. Bossy, M. Talmant, and P. Laugier, "Three-dimensional simulations of ultrasonic axial transmission velocity measurement on cortical bone models," The Journal of the Acoustical Society of America, vol. 115(5), pp. 2314-2324, 2004.